Edelweiss Applied Science and Technology
ISSN: 2576-8484
Vol. 9, No. 3, 2703-2712
2025
Publisher: Learning Gate
DOI: 10.55214/25768484.v9i3.5860

Biopolymer-based nanocomposites as antimicrobial agents for water purification

Anny Leudjo Taka[1], Mzimkhulu E. Monapathi[2*], Michael J. Klink[3]
[1,2,3]Department of Natural Sciences, Vaal University of Technology, Vanderbijlpark Campus,1900, South Africa; michaelk1@vut.ac.za (M.E.M.)

Abstract: The increasing antimicrobial resistance (AMR) caused by commonly used antimicrobial agents during wastewater treatment processes has prompted the use of nanomaterials as alternative antimicrobial agents. The present study aimed to determine the antimicrobial activity of biopolymer nanocomposites synthesized using a combination of phosphorylation and cross-linking polymerization techniques. The synthesized biopolymer nanocomposite, pCh-MWCNTs@Ag-TiO2, along with its intermediate product (pCh-MWCNTs), was characterized using spectroscopy, thermogravimetric analysis, and microscopy techniques. Antimicrobial assays were conducted using agar well diffusion and MIC. FTIR analysis confirmed the presence of key functional groups in the synthesized polymers, including phosphate groups, carbamate linkages, and the Ti-O-C bond in the pCh-MWCNTs@Ag-TiO_2 polymer. TGA revealed three thermal degradation stages: moisture and solvent loss, carbamate decomposition, and breakdown of MWCNTs and chitosan. BET analysis indicated that the pCh-MWCNTs polymer exhibited the largest surface area, SEM micrographs displayed a porous, spongy structure, and EDS confirmed the presence of elements such as C, O, P, Ag, and Ti. XRD patterns showed an amorphous structure, suggesting that nanomaterial incorporation disrupts the semi-crystalline nature of chitosan. Biopolymers exhibited antimicrobial activity against tested microorganisms. The developed pCh-MWCNT@Ag-TiO2 biopolymers were more effective, especially against S. aureus. The increasing incidence of waterborne pathogens and associated AMR in wastewater environments warrants further research on biopolymer-based nanocomposites.

Keywords: *Biopolymer, Cross-linking polymerization, Minimum inhibitory concentration nanocomposite, Well diffusion assay.*

1. Introduction

The use of nanomaterials in the form of biopolymer-based nanocomposites has received increased attention for water purification in the last decade [1, 2]. Nanocomposites are defined as polymer blends that incorporate non-toxic or low-toxicity nanomaterials. One example of a naturally derived polymer is chitosan recognized for its biocompatible properties such as being non-toxic, biodegradable, and environmentally friendly [3-6]. Biopolymer-based nanocomposites consist of multiple phases that incorporate nanoscale additives leading to their remarkable multifunctional properties. For instance, these nanocomposites can remove various pollutants from water especially microorganisms known to cause waterborne diseases [7, 8].

Research on the application of biopolymer-based nanocomposites as antimicrobial agents is still limited. Although several metal nanoparticles (NPs) have been used as antimicrobial agents, significant research limitations exist in the biocidal (antimicrobial) activity of biopolymer-based nanocomposites [3, 9]. One of the main reasons is that pathogenic microorganisms have developed resistance to conventional antibiotics [3]. There is a challenge to improve traditional water decontamination

History: Received: 15 January 2025; Revised: 19 March 2025; Accepted: 24 March 2025; Published: 29 March 2025
* Correspondence: michaelk1@vut.ac.za

techniques by designing new biopolymer-based nanocomposites with higher biocidal sensitivity and efficiency toward resistant pathogenic microorganisms.

Biopolymer-based nanocomposites can be created through *in-situ* and *ex-situ* methodologies. The *ex-situ* approach, often referred to as the physical method, entails first preparing nanoparticles (NPs) and then incorporating them into a polymer matrix, which acts as a dispersion medium. In contrast, the *in-situ* method, known as the chemical method, uses a polymer matrix, such as chitosan, to act as a capping agent or stabilizer. This is generally a preferred method because it controls the shape and size of the nanoparticles (NPs) and reduces NP agglomeration during the preparation process. Additionally, the *in-situ* method directly produces inorganic metal or metal oxide NPs within the polymer matrix solution, serving as the reaction medium. Examples of chemical methods include electrospinning, oxidation, sol-gel processes, cross-linking polymerization, precipitation, impregnation, and reduction [3, 4, 7, 10].

This research describes the development of a biopolymer nanocomposite composed of a phosphorylated chitosan cross-linked with multiwalled carbon nanotubes and doped with silver-titanium dioxide nanoparticles (pCh-MWCNTs@Ag-TiO_2) This was accomplished using a simple one-pot synthesis method through *in-situ* techniques. The objective of the current study was to assess the antimicrobial activity of the biopolymer nanocomposite against both Gram-positive and Gram-negative bacteria.

2. Materials and Methods

2.1. Synthesis of Biopolymer-Based Nanocomposites

The synthesis of the phosphorylated chitosan cross-linked with multiwalled carbon nanotubes and doped with silver-titanium dioxide nanoparticles (pCh-MWCNTs@Ag-TiO_2) utilized a hybrid approach that integrated both phosphorylation and cross-linking polymerization techniques. In the initial phase of this synthesis, 0.5 g of untreated chitosan was phosphorylated following the procedure outlined in Scheme 1 and a prior study Fatullayeva, et al. [11]. Then, pristine MWCNTs were oxidized by acid treatment as reported in the literature [12, 13].

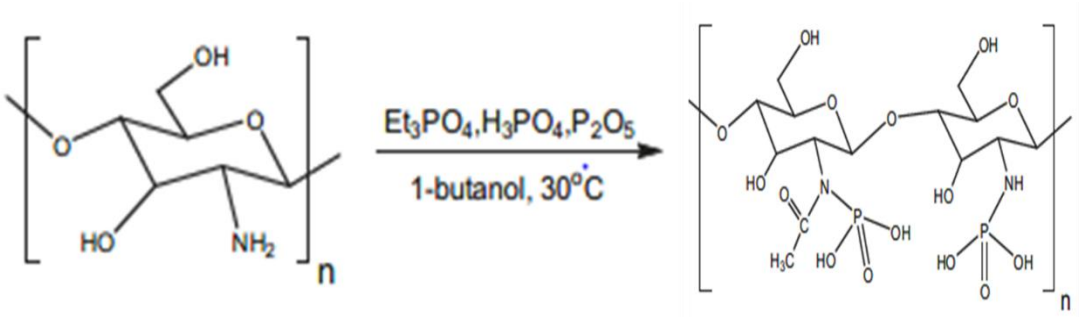

Figure 1.
Illustration of the phosphorylation reaction of chitosan [11].

In the second step, 0.251 g of phosphorylated chitosan (pCh) and 0.0140 g of oxidized MWCNTs were dispersed in 15 mL of dimethylformamide (DMF) (Sigma Aldrich, Johannesburg, South Africa) while stirring for 30 minutes in a nitrogen gas atmosphere. Subsequently, 4 mL of hexamethylene diisocyanate (HMDI) (Sigma Aldrich) was introduced to the reaction mixture at room temperature. The reaction temperature was then increased to 60°C, and the mixture was allowed to reflux for 24 hours. In an inert atmosphere, a solution containing 0.5 mL of TTIP and 0.0128 g of $AgNO_3$ (previously dispersed in 20 mL of DMF) was added to the polymer solution after the initial 24 hours of stirring. The polymerization reaction continued, refluxing at 60°C for another 24 hours. After this period, the polymerization reaction was stopped, and the solution was allowed to age for 3 days. An excess of acetone was added to the polymer solution to precipitate the product, and the mixture was refrigerated

Edelweiss Applied Science and Technology
ISSN: 2576-8484
Vol. 9, No. 3: 2703-2712, 2025
DOI: 10.55214/25768484.v9i3.5860

for 24 hours to ensure complete precipitation. The solution was then filtered to collect the precipitate, which was subsequently dried under a vacuum. The final product was obtained with a satisfactory yield of 3.87 g.

2.2. Characterization of Biopolymer-Based Nanocomposites

The biopolymer nanocomposite pCh-MWCNTs@Ag-TiO_2 and its intermediate product (pCh-MWCNTs) were characterized using the Brunauer-Emmett-Teller (BET) method, thermogravimetric analysis (TGA), and spectroscopy techniques. Furthermore, scanning electron microscopy combined with energy-dispersive X-ray (SEM-EDX) spectroscopy was utilized in the characterization process.

A Micromeritics Tristar 3000 surface and porosity analyser was used for Brunauer-Emmett-Teller (BET) analysis. Before the analysis, approximately 0.25 g of the sample was degassed under nitrogen at 60°C for 4 hours. Fourier-transform infrared (FTIR) analysis was conducted using a Spectrum 100 Perkin Elmer spectrophotometer to assess the various functional groups and interactions present in the prepared polymer samples. This analysis involved the preparation of pellet samples for evaluation. X-ray diffraction (XRD) was performed using a Rigaku Ultima IV X-ray diffractometer with copper Kα radiation (40 kV, 30 mA, wavelength = 0.154 nm). Furthermore, a Pyris Series-TGA 4000 analyser was employed to assess the thermal stability of the synthesized samples under nitrogen gas (20 ml/min) at a heating rate of 10°C/min.

2.3. Antimicrobial Activity Studies

2.3.1. Antimicrobial Susceptibility Screening by Agar Well Diffusion

The agar well diffusion method [14] was utilized to evaluate the effectiveness of the biopolymers against two test bacterial species: *Escherichia coli* ATCC 14169 (Gram-negative) and *Staphylococcus aureus* ATCC 25923 (Gram-positive). The inoculum was prepared by incubating the test organisms for 24 hours at 37°C in Mueller-Hinton Broth (MHB) (Biolab Merck, city, Germany) on a shaker at 150 rpm to achieve final inoculum concentrations of approximately 10⁶ CFU/mL. Exactly 100 uL of the inoculum was then spread onto Mueller-Hinton Agar (Biolab Merck) plates. Wells (diameter = 6 mm, depth = 4 mm) were aseptically created in the agar, and 30 µL of the biopolymers (at concentrations of 7 mg/mL, 3.5 mg/mL, and 1.75 mg/mL) were added separately to the wells. Neomycin (0.1 mg/mL) was used as the positive control, while sterile MHB was used as the negative control. The antimicrobial activity of the biopolymers against the test organisms was indicated by the formation of a clear zone of inhibition (measured in mm) around the wells after 24 hours of incubation at 37°C.

2.4. Minimum Inhibitory Concentrations

The antimicrobial activity of the biopolymers against the test organisms was quantitatively assessed using Minimum Inhibitory Concentrations (MICs). Fresh inoculants of the test organisms were prepared from 24 hours of shaking incubation at 37°C in Mueller-Hinton Broth. A twofold dilution of the biopolymers (7 mg/mL, 3.5 mg/mL, and 1.75 mg/mL) was performed in duplicate in 96-well plates. Positive control (neomycin at 0.1 mg/mL) and negative control (sterile MHB) were included as references. Exactly 100 uL of the overnight-grown cultures were added to the wells and incubated for 24 hours at 37°C. Bacterial growth was assessed using 0.02% resazurin dye, followed by an additional incubation at 37°C for 24 hours. The plates were then examined for a colour change from blue to pink. The MIC endpoint was defined as the lowest concentration at which a colour change was observed.

3. Results and Discussion

3.1. Synthesis and Characterization

The thermogravimetric analysis (TGA) curves of the biopolymer nanocomposites developed in this study are shown in Figure. 2. TGA analysis was used to investigate the thermal stability of the

Edelweiss Applied Science and Technology
ISSN: 2576-8484
Vol. 9, No. 3: 2703-2712, 2025
DOI: 10.55214/25768484.v9i3.5860

synthesized polymers. The results indicated three distinct phases of thermal decomposition. The first phase, occurring between 50°C and 200°C, is associated with the loss of moisture, and solvents present in the synthesized biopolymer nanocomposites. The next phase, ranging from 250°C to just below 400°C, represents the decomposition of the carbamate groups within the polymer. Lastly, the third phase (from 400°C and above) is associated with the breakdown of the multiwalled carbon nanotubes (MWCNTs) within the polymers and the complete degradation of the chitosan polymer.

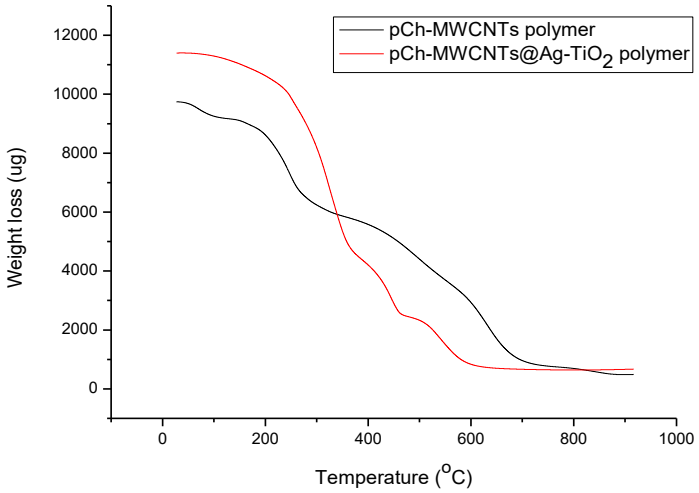

Figure 2.
TGA curves of the developed biopolymer nanocomposites.

framework. Figure 3 illustrates the FTIR spectra of the synthesized biopolymer nanocomposites. FTIR analysis was performed to confirm the presence of various functional groups and interactions in the synthesized polymers. Notably, interactions such as amide linkages, hydrogen bonding, and several oxygen-containing groups were easily identified during the spectral analysis. For example, phosphate groups, including the P=O stretch at 1110 cm^{-1} and the P-O stretch at 1090 cm^{-1}, were observed. The presence of the carbamate linkage NH(CO), indicative of polymerization, was observed around 1685 cm^{-1} and 1530 cm^{-1}. The peak at 1380 cm^{-1} was associated with the Ti-O-C group in the pCh-MWCNTs@Ag-TiO_2 polymer. Bending vibrations of C-H in the aromatic group were detected around 2067 cm^{-1} and 2000 cm^{-1}. The peaks at 2933 cm^{-1} and 2860 cm^{-1} were attributed to asymmetric and symmetric C-H stretching in CH_2 groups bonded to oxygen. A strong absorption band in the range of 3443 cm^{-1} to 3337 cm^{-1} was linked to O-H and N-H stretching vibrations. Furthermore, these electron-rich functional groups facilitate pollutant removal through various mechanisms [2, 12].

Edelweiss Applied Science and Technology
ISSN: 2576-8484
Vol. 9, No. 3: 2703-2712, 2025
DOI: 10.55214/25768484.v9i3.5860

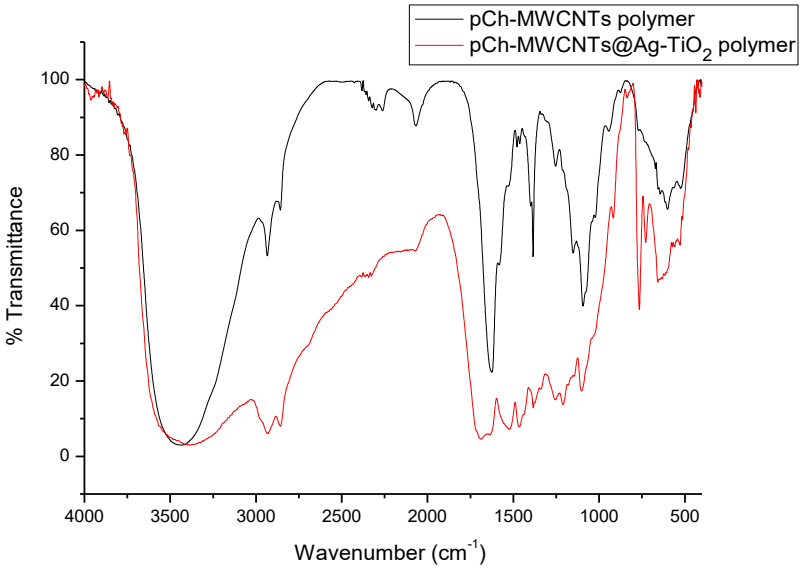

Figure 3.
FTIR spectra of the synthesized biopolymer nanocomposites.

The BET results for the synthesized biopolymer nanocomposites are shown in Table 1. The surface area and pore size of the developed polymers were evaluated using BET analysis. The findings revealed that the surface area of the synthesized biopolymer nanocomposites was generally low. This reduced surface area may be attributed to the stringent degassing conditions which affected the materials before the BET analysis. However, it is important to note that the pCh-MWCNTs polymer demonstrated the highest surface area. Any reason for this?

Table 1.
Summary of the results from the BET surface area analysis.

Nano-adsorbent Polymers	Surface Area (m^2 / g)	Pore size (nm)
pCh-MWCNT@Ag-TiO_2	0.5784	1811.7
pCh-MWCNT	7.4696	15688

The SEM micrographs of the biopolymer nanocomposites are shown in Figure. 4. The surface morphologies of these biopolymer nanocomposites show a porous and spongy material structure. Simultaneously, EDS analysis was conducted to confirm the elemental composition of the synthesized biopolymer nanocomposite. The EDS spectrum of pCh-MWCNTs@Ag-TiO_2 (Figure. 5) reveals the presence of elements such as C, O, P, Ag, and Ti.

Edelweiss Applied Science and Technology
ISSN: 2576-8484
Vol. 9, No. 3: 2703-2712, 2025
DOI: 10.55214/25768484.v9i3.5860

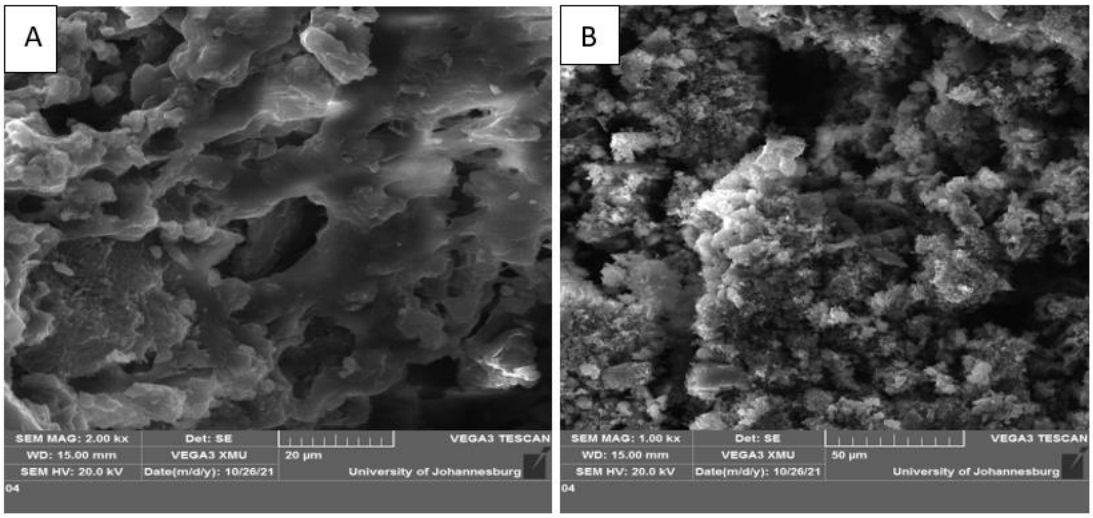

Figure 4.
SEM micrographs of (A) pCh-MWCNTs@Ag-TiO2 and (B) pCh-MWCNTs.

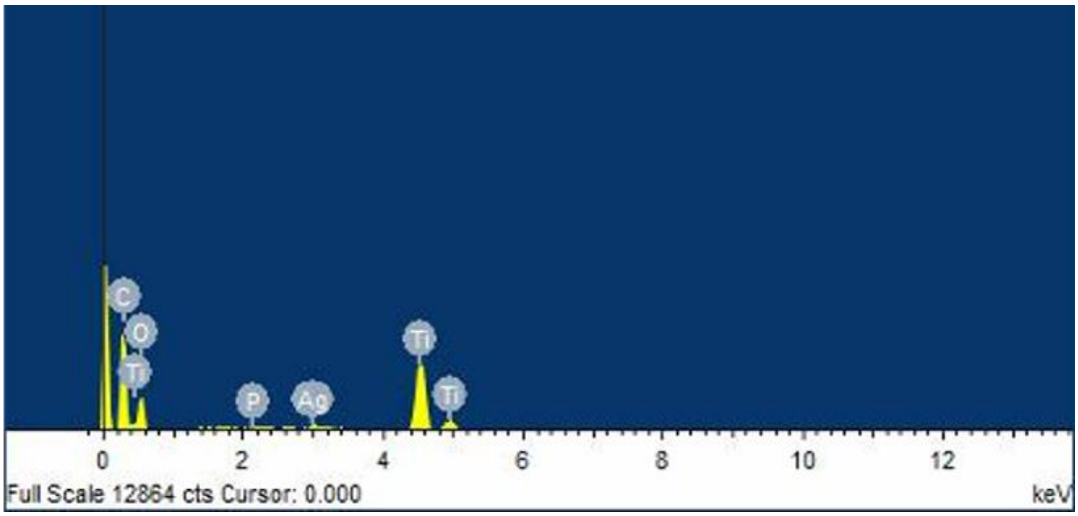

Figure 5.
EDS spectrum of pCh-MWCNTs@Ag-TiO2.

Edelweiss Applied Science and Technology
ISSN: 2576-8484
Vol. 9, No. 3: 2703-2712, 2025
DOI: 10.55214/25768484.v9i3.5860

Figure 6 presents the XRD patterns of the biopolymer nanocomposites. XRD analysis was conducted to assess the purity and crystallinity of the prepared polymers. Only a few crystalline peaks were observed in the XRD patterns of the pCh-MWCNTs polymer and phosphorylated chitosan. The prominent peaks in the figure are broad and indicative of an amorphous nature suggesting that chitosan exhibits semi-crystalline properties; however, the incorporation of additional nanomaterials through functionalization disrupts the crystallinity within the chitosan polymer chain.

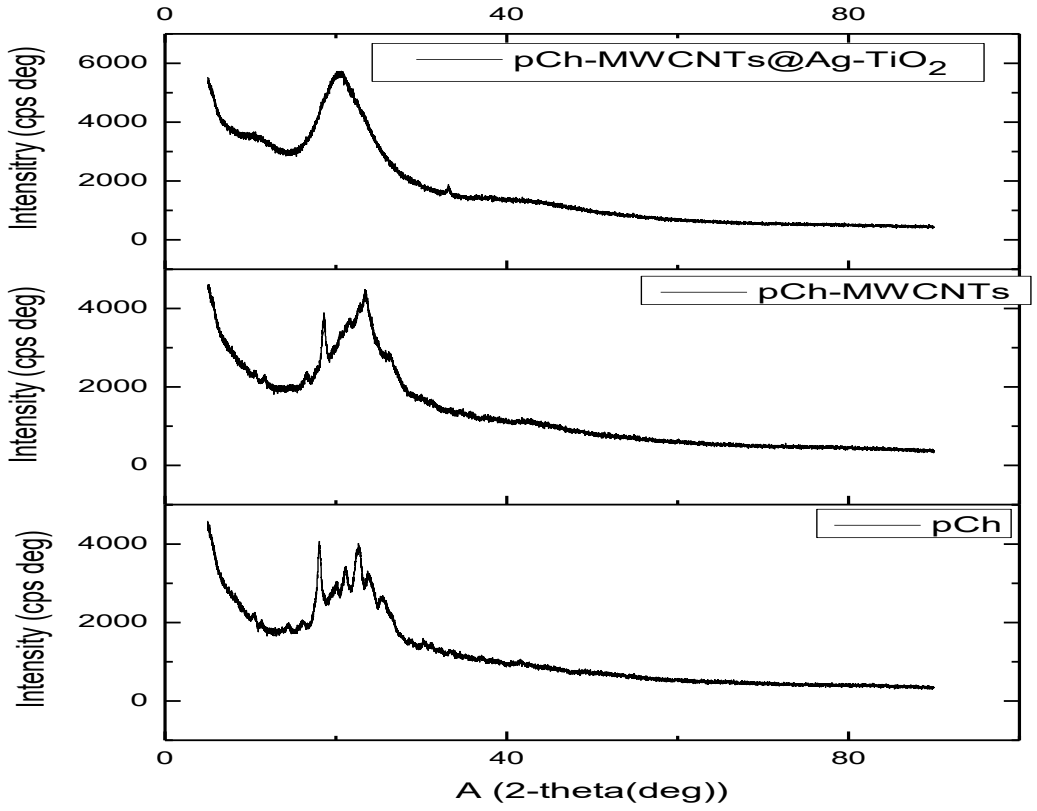

Figure 6.
XRD patterns of the developed polymers.

3.2. Antimicrobial Susceptibility Tests

3.2.1. Agar Well Diffusion Assay

The agar well diffusion results showed varying antimicrobial activity for the two biopolymers against the two test organisms. Figure 7a displays the zone of inhibition (the clear area around microbial growth) which indicates the antimicrobial activity of the biopolymer.

Edelweiss Applied Science and Technology
ISSN: 2576-8484
Vol. 9, No. 3: 2703-2712, 2025
DOI: 10.55214/25768484.v9i3.5860

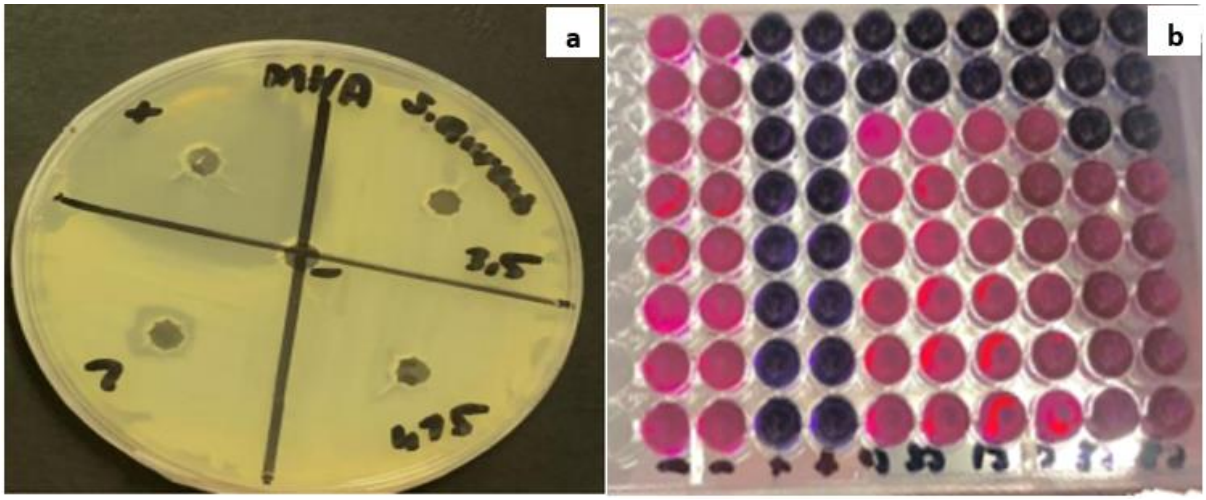

Figure 7.
An indication of antimicrobial activity of developed pCh-MWCNTs@Ag-TiO2 against the test organisms: (a) Formation of a zone of inhibition on an agar plate around an antimicrobial agent (b) Minimum inhibitory concentration indicated by colour changes.

The diameters of the clear zones of inhibition are shown in Table 2. No clear zones were observed for pCh-MWCNTs@Ag-TiO_2 and the intermediate product, pCh-MWCNTs, except for the former at a concentration of 7 mg/mL against *S. aureus*. This confirms that pCh-MWCNTs@Ag-TiO_2 (7 mg/mL) was more effective than pCh-MWCNTs against *S. aureus*. Both polymers were not effective against *E. coli* at all predetermined concentrations.

Gram-negative bacteria have an outer membrane that acts as a barrier and prevents many antibiotics from reaching their intracellular targets [15]. Thus, may be a reason why the polymers were not effective against *E. coli*. Effective antimicrobial agents should infiltrate a microorganism's outer membrane and damage the microbial DNA and protein [16].

Table 2.
Mean diameters of zone of inhibition from agar well diffusion assay.

Agar well diffusion								
Test organisms	**Mean zones of inhibition (mm)**							
	pCh-MWCNTs (mg/mL)			**pCh-MWCNTs@Ag-TiO_2 (mg/mL)**			**Positive control (Neomycin)**	**Negative control (sterile MHB)**
	7	3.5	1.75	7	3.5	1.75		
E. coli	0	0	0	0	0	0	26	0
S. aureus	0	0	0	10	0	0	38	0

3.3. Minimum Inhibitory Concentrations

The antimicrobial activity of the biopolymer nanocomposite was quantitatively assessed using MIC which determines the lowest concentration at which the antimicrobial agent could completely inhibit visible growth of a microorganism under controlled *in vitro* conditions [17]. The colour change from blue to pink (Figure. 7b) indicates chemical reduction from aerobic respiration due to cell growth [18]. The addition of the resazurin dye serves to confirm cell viability through this colour change. The persistent blue colour of the indicator dye signifies that the biopolymer nanocomposite effectively inhibits microbial activity [19].

Table 3. shows MIC endpoints for the biopolymer against the test microorganisms. Unlike the qualitative agar well diffusion method which did not show the actual antimicrobial activity, the quantitative MIC technique showed the Minimum inhibitory concentrations at which the polymers could exert their antimicrobial effectiveness. The lower the MIC, the more effective the antimicrobial

Edelweiss Applied Science and Technology
ISSN: 2576-8484
Vol. 9, No. 3: 2703-2712, 2025
DOI: 10.55214/25768484.v9i3.5860

agent [20]. Minimum inhibitory concentrations in the current study ranged from 7 to 0.4375 mg/mL for the biopolymer-based nanocomposite.

Table 3 shows lower MIC values for all the concentrations (7 mg/mL, 3.5 mg/mL, and 1.75 mg/mL) for pCh-MWCNTs@Ag-TiO_2 compared to its intermediate product, pCh-MWCNTs. Furthermore, the MIC values for pCh-MWCNTs@Ag-TiO_2 were lower for *S. aureus* (0.4375 mg/mL) than for *E. coli.* (0.875 mg/mL). Table 2 shows no antimicrobial activity at any concentration except for 7 mg/mL of pCh-MWCNTs@Ag-TiO2 against *S. aureus.* Kowalska-Krochmal and Dudek-Wicher [21] stipulated an inverse correlation between zones of inhibition in the Agar well diffusion technique and associated MICs. An inverse correlation was observed for biopolymer-based nanocomposites (7 mg/mL) activity against *S. aureus*, where a larger mean zone of inhibition (10 mm) and lowest MIC value were observed. Additionally, as shown in Table 2, Neomycin was more effective than the biopolymer nanocomposites. This is also confirmed by low MIC values in Table 3.

Table 3.
Minimum inhibitory concentrations of biopolymer-based nanocomposites.

Minimum inhibitory concentrations								
Test organisms	**MIC endpoints**							
	pCh-MWCNTs (mg/mL)			**pCh-MWCNTs@Ag-TiO_2 (mg/mL)**			**Positive control (Neomycin)**	**Negative control (sterile MHB)**
	7	3.5	1.75	7	3.5	1.75		
E. coli	7	3.5	1.75	3.5	1.75	0.875	<0.0156	No inhibition
S. aureus	3.5	1.75	0.875	3.5	1.75	0.4375	<0.0156	No inhibition

4. Conclusion

The emergent antimicrobial resistance against conventional antimicrobial drugs shows an urgent need for alternative treatment approaches. In the present study, the biopolymer nanocomposite pCh-MWCNT@Ag-TiO_2 was successfully synthesized and characterized. Both the intermediate pCh-MWCNTs and developed pCh-MWCNT@Ag-TiO_2 biopolymer displayed antimicrobial activity against bacteria found in wastewater. The developed pCh-MWCNT@Ag-TiO_2 biopolymer nanocomposite should be tested against a larger pool of Gram-positive and Gram-negative bacteria.

Funding:

The authors thank the financial support of the National Research Fund (NRF) (Grant number: PDG200408511608) in South Africa. and the South African Weather Services (SAWS), South Africa. The authors also acknowledge the help of the Department of Natural Sciences at Vaal University of Technology and the Institute of Chemical and Biotechnology, South Africa for their research laboratories. The views expressed are those of the authors and not of the funding agency.

Transparency:

The authors confirm that the manuscript is an honest, accurate, and transparent account of the study; that no vital features of the study have been omitted; and that any discrepancies from the study as planned have been explained. This study followed all ethical practices during writing.

References

[1] A. L. Taka, K. Pillay, and X. Y. Mbianda, "Nanosponge cyclodextrin polyurethanes and their modification with nanomaterials for the removal of pollutants from waste water: A review," *Carbohydrate Polymers*, vol. 159, pp. 94-107, 2017. https://doi.org/10.1016/j.carbpol.2016.12.053

[2] A. L. Taka, E. Fosso-Kankeu, K. Pillay, and X. Y. Mbianda, "Removal of cobalt and lead ions from wastewater samples using an insoluble nanosponge biopolymer composite: adsorption isotherm, kinetic, thermodynamic, and regeneration studies," *Environmental Science and Pollution Research*, vol. 25, pp. 21752-21767, 2018. https://doi.org/10.1007/s11356-018-2055-6

[3] L. A. Taka, E. Fosso-Kankeu, E. B. Naidoo, and X. Yangkou Mbianda, "Recent development in antimicrobial activity of biopolymer-inorganic nanoparticle composites with water disinfection potential: A comprehensive review," *Environmental Science and Pollution Research*, vol. 28, pp. 26252-26268, 2021. https://doi.org/10.1007/s11356-021-13373-z

[4] A. L. Taka, M. J. Klink, X. Y. Mbianda, and E. B. Naidoo, "Chitosan nanocomposites for water treatment by fixed-bed continuous flow column adsorption: A review," *Carbohydrate Polymers*, vol. 255, p. 117398, 2021. https://doi.org/10.1016/j.carbpol.2020.117398

[5] E. Akdaşçi, H. Duman, F. Eker, M. Bechelany, and S. Karav, "Chitosan and its nanoparticles: A multifaceted approach to antibacterial applications," *Nanomaterials*, vol. 15, no. 2, p. 126, 2025. https://doi.org/10.3390/nano15020126

[6] F. Mohammad, H. A. Al-Lohedan, and H. N. Al-Haque, "Chitosan-mediated fabrication of metal nanocomposites for enhanced biomedical applications," *Advanced Materials Letters*, vol. 8, no. 2, pp. 89-100, 2017. https://doi.org/10.5185/amlett.2017.6925

[7] M. Alsuhybani, A. Alshahrani, and A. S. Haidyrah, "Synthesis, characterization, and evaluation of evaporated casting MWCNT/chitosan composite membranes for water desalination," *Journal of Chemistry*, vol. 2020, no. 1, p. 5207680, 2020. https://doi.org/10.1155/2020/5207680

[8] G. Ö. Kayan and A. Kayan, "Composite of natural polymers and their adsorbent properties on the dyes and heavy metal ions," *Journal of Polymers and the Environment*, vol. 29, no. 11, pp. 3477-3496, 2021. https://doi.org/10.1007/s10924-021-02085-5

[9] A. L. Taka *et al.*, "Spectroscopic characterization and antimicrobial activity of nanoparticle doped cyclodextrin polyurethane bionanosponge," *Materials Science and Engineering: C*, vol. 115, p. 111092, 2020. https://doi.org/10.1016/j.msec.2020.111092

[10] J. Yang *et al.*, "Nanomaterials for the removal of heavy metals from wastewater," *Nanomaterials*, vol. 9, no. 3, p. 424, 2019. https://doi.org/10.3390/nano9030424

[11] S. Fatullayeva, D. Tagiyev, N. Zeynalov, S. Mammadova, and E. Aliyeva, "Recent advances of chitosan-based polymers in biomedical applications and environmental protection," *Journal of Polymer Research*, vol. 29, no. 7, p. 259, 2022. https://doi.org/10.1007/s10965-022-02911-1

[12] A. Leudjo Taka, K. Pillay, and X. Y. Mbianda, *Synthesis and characterization of a novel bio nanosponge filter (pMWCNT-CD/TiO 2-Ag) as potential adsorbent for water purification* (Emerging Trends in Chemical Sciences). Springer International Publishing. https://doi.org/10.1007/978-3-319-69036-7_14, 2018.

[13] N. Sezer and M. Koç, "Oxidative acid treatment of carbon nanotubes," *Surfaces and Interfaces*, vol. 14, pp. 1-8, 2019. https://doi.org/10.1016/j.surfin.2018.11.002

[14] G. Moukangoe *et al.*, "Synthesis and antibacterial activity of Cobalt-thiourea nanoparticles on selected waterborne bacterial pathogens," *Digest Journal of Nanomaterials and Biostructures*, vol. 15, pp. 757-766, 2020.

[15] K. L. May and M. Grabowicz, "The bacterial outer membrane is an evolving antibiotic barrier," *Proceedings of the National Academy of Sciences*, vol. 115, no. 36, pp. 8852-8854, 2018. https://doi.org/10.1073/pnas.1810882115

[16] S. I. Siddiqui, O. Manzoor, M. Mohsin, and S. A. Chaudhry, "Nigella sativa seed based nanocomposite-MnO2/BC: An antibacterial material for photocatalytic degradation, and adsorptive removal of Methylene blue from water," *Environmental Research*, vol. 171, pp. 328-340, 2019. https://doi.org/10.1016/j.envres.2019.01.041

[17] C. I. Owuama, "Determination of minimum inhibitory concentration (MIC) and minimum bactericidal concentration (MBC) using a novel dilution tube method," *African Journal of Microbiological Research*, vol. 11, no. 23, pp. 977-980, 2017.

[18] F. Bonnier *et al.*, "Cell viability assessment using the Alamar blue assay: A comparison of 2D and 3D cell culture models," *Toxicology in Vitro*, vol. 29, no. 1, pp. 124-131, 2015.

[19] N. Mabungela *et al.*, "Multi-application fennel-based composites for the adsorption of Cr (VI) ions from water and control of Escherichia coli and Staphylococcus aureus," *Environmental Chemistry and Ecotoxicology*, vol. 4, pp. 171-185, 2022.

[20] M. J. Klink, N. Laloo, A. Leudjo Taka, V. E. Pakade, M. E. Monapathi, and J. S. Modise, "Synthesis, characterization and antimicrobial activity of zinc oxide nanoparticles against selected waterborne bacterial and yeast pathogens," *Molecules*, vol. 27, no. 11, p. 3532, 2022. https://doi.org/10.3390/molecules27113532

[21] B. Kowalska-Krochmal and R. Dudek-Wicher, "The minimum inhibitory concentration of antibiotics: Methods, interpretation, clinical relevance," *Pathogens*, vol. 10, no. 2, p. 165, 2021. https://doi.org/10.3390/pathogens10020165

Edelweiss Applied Science and Technology
ISSN: 2576-8484
Vol. 9, No. 3: 2703-2712, 2025
DOI: 10.55214/25768484.v9i3.5860